

of reference 1, which can be written for hcp ^3He
 $T_{\text{EL}}^{-1} = 1.55 \times 10^{-35} (d^2 J / da^2)^2 T^7 / \theta_D^{10} \text{ sec}^{-1}$, (12)

(in which a is the nearest-neighbor distance and θ_D the Debye temperature of the solid), and our measurements accurately confirm the T^7 temperature dependence,⁵ as is indicated in Fig. 3.

We are grateful to A. G. Redfield for his critical reading of the manuscript and to J. Krueger for measuring photographs.

Note added in proof.—After submission of this note we received a preprint by Beal, Gifford, Hatton, Richards, and Richards describing similar work on several ^3He - ^4He mixtures of low ^4He concentration. Our results were obtained on ^3He containing 0.95% ^4He .

¹R. L. Garwin and A. Landesman, Phys. Rev. **133**, A1503 (1964). We believe the present measurements are the first accurate observations of this relaxation rate, which varies as T^{-7} .

²H. A. Reich, Phys. Rev. **129**, 630 (1963). The numerical values of J in this paper are, in part, erroneous. We believe the data of this experiment appears properly interpreted in reference 1.

³D. O. Edwards, A. S. McWilliams, and J. G. Daunt, Phys. Letters **1**, 218 (1962).

⁴G. O. Zimmerman, H. A. Fairbank, M. Strongin, and B. T. Bertman, Bull. Am. Phys. Soc. **8**, 91 (1963).

⁵One might question the consistency between our results for $T_{\text{EL}} \propto T^{-7}$ as published here in Fig. 3 for hcp ^3He and the essentially Curie-law susceptibility for bcc ^3He published in Figs. 2 and 3 of A. L. Thomson, H. Meyer, and P. N. Dheer, Phys. Rev. **132**, 1455 (1963). These latter indicate "prompt" cooling of the spin system to $\sim 0.06^\circ\text{K}$ in ^3He of molar volume 22.40 and 24.3 cm^3/mole . There is no discrepancy—first, the T_{EL} of Eq. (12) varies $\propto V^{-60}$ (locally); and, second, at low temperatures the Raman relaxation is slow compared with the single-phonon relaxation process calculated in R. B. Griffiths, Phys. Rev. **124**, 1023 (1961). To illustrate these points we have calculated T_{EL} for bcc ^3He of $V = 24.3 \text{ cm}^3/\text{mole}$. We find from the theory, $T_{\text{EL}}^{-1} = (2.0 \times 10^4 T^7 + 0.5 T) \text{ sec}^{-1}$. At 0.06°K , this material thus has $T_{\text{EL}} \sim 30 \text{ sec}$, and about 5 msec at 0.5°K .

INTERACTION BETWEEN HELICON WAVES AND SOUND WAVES IN POTASSIUM

C. C. Grimes and S. J. Buchsbaum

Bell Telephone Laboratories, Murray Hill, New Jersey

(Received 24 February 1964)

The possibility of observing an interaction between helicon waves¹ and transverse sound waves in a metal has been recently considered by several authors.²⁻⁴ The coupling is expected to occur when the helicon-wave phase velocity is nearly equal to the sound-wave phase velocity. We report here the results of experiments designed to measure such coupling in pure, single-crystal potassium. As shown in Figs. 1 and 2, we obtained clear evidence of the existence of the interaction and found good agreement between theory and experiment.

The dispersion relation for coupled helicon waves and sound waves in an elastically isotropic medium has been derived in references 2 through 4. The analysis used there is similar to that previously employed for study of acoustic attenuation in metals.⁵ In order to interpret the results of our experiment, it was necessary to derive a more general dispersion relation applicable to the elastically anisotropic case of wave propagation along a twofold axis. We take as

our model an infinite medium having n free electrons per cm^3 and a positive (ion) background of charge density ne and mass density nM . Take the magnetic field \vec{H}_0 to be in the z direction and assume that all field quantities vary as $e^{i(kz - \omega t)}$. Denote right- and left-circularly polarized field quantities by $E^\pm = E_x \pm iE_y$, $J^\pm = J_x \pm iJ_y$, etc. The equation of motion of the positive background becomes

$$\omega^2 \vec{S}^\pm = v_1^2 k^2 \frac{1}{2} (\vec{S}^+ + \vec{S}^-) \pm v_2^2 k^2 (\vec{S}^+ - \vec{S}^-) - (e/M) \vec{E}^\pm - (e/Mc) \dot{\vec{S}}^\pm \times \vec{H}_0 + (e/M\sigma_0) (\vec{J}^\pm + \vec{j}^\pm), \quad (1)$$

where \vec{S}^\pm is the displacement of an ion from its equilibrium position, τ is the electron relaxation time, $\vec{J}^\pm = ne \dot{\vec{S}}^\pm$ is the current density due to motion of the ions, \vec{j}^\pm is the electron current density, \vec{E}^\pm is the internal electric field, and $\sigma_0 = ne^2 \tau / m$; v_1 and v_2 are the phase velocities of the two independent shear waves when they propagate along the twofold direction in the absence of a magnetic field. Equation (1) exhibits

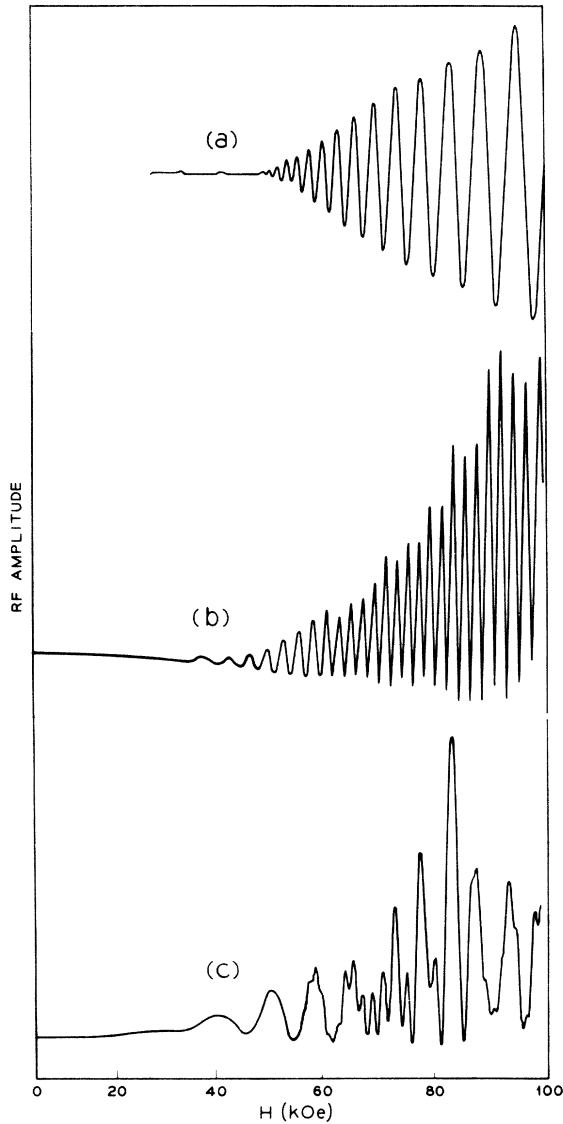


FIG. 1. Experimental curves showing the rf amplitude across the receiver coil as a function of applied magnetic field. Curve (a), obtained in sodium, represents "pure" helicon wave propagation and is to be contrasted with curves (b) and (c) which represent helicon waves interacting with sound waves in single-crystal potassium. The beat pattern occurs because the signals from the two coupled waves transmitted through the specimen are added to a reference signal which has fixed amplitude and phase. Maxima occur when the signal from a transmitted wave is in phase with the reference signal.

the fact that when v_1 and v_2 are unequal, the normal modes of propagation are elliptically polarized waves with the degree of ellipticity being a function of \vec{H}_0 . Proceeding very much as in reference 4, we can derive the dispersion

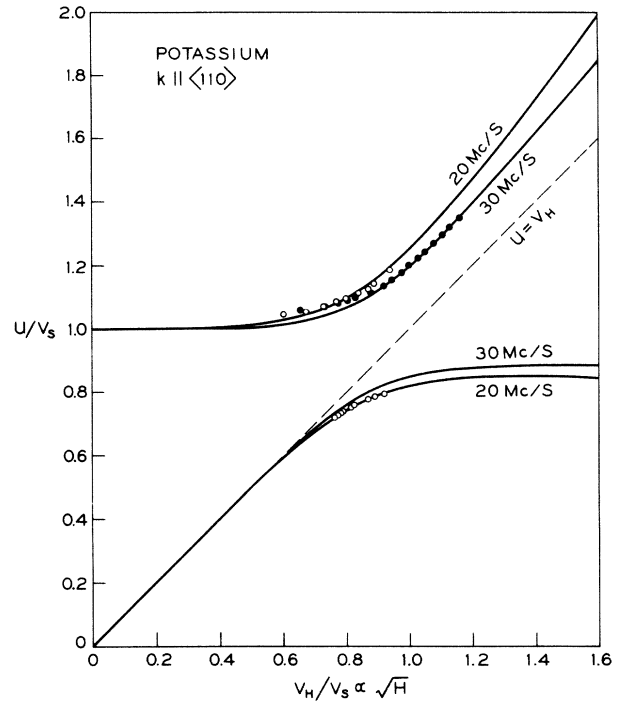


FIG. 2. Comparison of the calculated dispersion curves with data points deduced from the experimental curves shown in Figs. 1(b) and 1(c). The quantity u/v_s plotted along the ordinate is the phase velocity of an excitation normalized to the velocity of sound, while the quantity $v_H/v_s \propto \sqrt{H}$ plotted along the abscissa is proportional to the square root of the magnetic field intensity. The lower branches of the dispersion relation represent excitations which are helicon waves for $v_H/v_s \ll 1$ and become sound waves for $v_H/v_s \gg 1$. The upper branches change from sound waves to helicon waves with increasing v_H/v_s .

relation for the coupled system of transverse electromagnetic and sound waves. The dispersion relation in its full generality is lengthy and will be discussed in a future publication. For the discussion of the present experiment it is sufficient to neglect collisions ($\tau \rightarrow \infty$),⁶ to assume a local relationship between field and current ($\omega_c \gg kv_{\text{Fermi}}$), to neglect the displacement current, and to set $\omega \ll \omega_c$. The dispersion relation can then be written in the form

$$\begin{aligned} & \{ (v_H^2/u^2 + 1)(v_2^2/u^2 - 1 + \Omega/\omega) - \Omega/\omega \} \\ & \times \{ (v_H^2/u^2 - 1)(v_1^2/u^2 - 1 - \Omega/\omega) - \Omega/\omega \} \\ & = (\Omega/\omega)(v_H^4/u^4)[(v_1^2 - v_2^2)/u^2], \end{aligned} \quad (2)$$

where $u = \omega/k$, $\Omega = eH_0/Mc$, and $v_H^2 = c^2 m \omega \omega_C / 4\pi n e^2$ is the squared phase velocity of a "pure" helicon wave. Solutions of Eq. (2) for $u \leq v_1$ are plotted as the solid curves in Fig. 2.

The term on the right-hand side of Eq. (2) couples the right- and left-circularly polarized components and leads to elliptically polarized waves. If $v_1 = v_2$, the right-hand side vanishes and the two circularly polarized components become independent as was found in references 2 through 4. When $v_1 = v_2$, there are three real roots of Eq. (2) corresponding to right- and left-circularly polarized sound waves and the right-circularly polarized helicon wave. The term Ω/ω acts as a coupling parameter which couples the helicon wave and the right-circularly polarized sound wave. In the interaction region where $v_H \approx v_1$, we can write the coupling parameter in the form

$$(\Omega/\omega) v_H \approx v_1 = (H^2/4\pi C_{ij}), \quad (3)$$

where C_{ij} is the combination of elastic constants satisfying the relation $v_1^2 = C_{ij}/nM$. Thus to observe the strongest possible coupling of the helicon and sound waves, the interaction should be studied at the highest attainable magnetic field and in a crystal having the smallest possible stiffness modulus. These considerations led us to select potassium as the most favorable material in which to observe the interaction. Further consideration reveals that C_{ij} is a minimum for the shear wave propagating in the [110] direction and having particle motion in the $[1\bar{1}0]$ direction. For this case, the coupling parameter

$$(\Omega/\omega) v_H \approx v_1 \approx 0.2 \text{ for } H_0 \approx 10^5 \text{ G.}$$

The experimental configuration we have employed consists of a transmitter coil and a receiver coil in close proximity to the opposite faces of a slab-shaped specimen ($2.5 \times 2.5 \times 0.3$ cm). Currents from a radio-frequency oscillator flow in the transmitter coil and induce currents in the surface of the specimen. The rf currents propagate in the helicon mode through the specimen to the opposite surface where some of the transmitted energy is coupled into the receiver coil. The signal from the receiver coil is amplified, rectified, and plotted as a function of \vec{H}_0 on the X-Y recorder. Sufficient stray input signal is coupled into the receiver coil to provide a reference signal whose phase and am-

plitude are independent of \vec{H}_0 . The reference signal and the signal transmitted through the sample add vectorially to produce a beat pattern consisting of maxima and minima when the two signals are in and out of phase, respectively. The beat pattern provides a convenient means of determining the change in phase of the transmitted waves as \vec{H}_0 is varied. This experimental technique allows detection of traveling waves in addition to detection of standing-wave resonances.⁷

In Fig. 1 are shown three experimentally obtained traces of the transmitted signal as a function of H_0 . Curve (a) was obtained in a polycrystalline sodium slab 0.048 cm thick at 50 Mc/sec. Since in sodium there is no interaction with the sound wave over the range of H_0 used, curve (a) is a signature of a "pure" helicon wave and is included for contrast with curves (b) and (c). The most important feature of curve (a) is the monotonic increase in the separation between successive maxima as H_0 is increased which results from the fact that $v_H^2 \propto H_0$. Curves (b) and (c) of Fig. 1 are for wave propagation in the [110] direction in potassium at frequencies of 30 and 20 Mc/sec, respectively, and a temperature of 4.2°K. At the higher frequency [curve (b)], the coupling between the helicon and sound waves is relatively weak and manifests itself by an increasing separation of the successive maxima as the magnetic field is decreased at low values, that is, a less rapid slow-down with decreasing magnetic field of the phase velocity of the wave than that dictated by the "pure" helicon wave formula. Here only the upper branch of the dispersion relation of Fig. 2 is discernible. In curve (c), at 20 Mc/sec, the coupling is sufficiently strong for both waves to appear, that is, the beat pattern in Fig. 1(c) can be resolved into two series of peaks corresponding to two coupled branches of the dispersion relation. The series of peaks that are widely spaced at lower fields and become more closely spaced at higher fields belong to a branch of the dispersion relation that resembles a sound wave at low fields and a helicon wave at high fields. The second series of peaks becomes more widely spaced with increasing H_0 and belongs to a branch of the dispersion relation which is changing from a helicon wave to a sound wave.

Data points deduced from the experimental curves in Figs. 1(b) and 1(c) are compared with theoretical curves in Fig. 2. The theoretical curves were calculated from Eq. (2) taking $v_1 = v_S = 7 \times 10^4$ cm/sec and $v_2 = 1.75 \times 10^5$ cm/sec.⁸

In this plot a pure helicon wave would be represented by the straight dashed line $u/v_S = v_H/v_S$. We see that the lower branches of the dispersion relation represent excitations which are helicon waves for $v_H/v_S \ll 1$ and which resemble sound waves for $v_H/v_S \gg 1$. The upper branches represent excitations which change from sound waves for $v_H/v_S \ll 1$ to helicon waves for $v_H/v_S \gg 1$. The experimental data points contain an adjustable parameter in the following sense: The magnitude of the wave number, k , corresponding to a given peak is not accurately known. However, in a series of peaks in the beat pattern two successive peaks differ in wave number by $2\pi/d$, where d is the thickness of the specimen. Since k decreases with increasing H_0 , we arbitrarily assign a k value to one, and only one, peak in each series of peaks. In Fig. 2 we have arbitrarily assigned a k value to that peak in each series of peaks which appears at the highest magnetic field. In each case the k value was chosen to make the data point lie near the corresponding theoretical curve. The adjustable parameter enters essentially as a translation of each series of data points along the ordinate in Fig. 2. Consequently, the data points are to be compared only with the slope and curvature of the theoretical curves.

From a study of the 20- and 30-Mc/sec data discussed here and additional data obtained at frequencies ranging from 5 Mc/sec to 50 Mc/sec, we conclude that the coupling of helicon waves and transverse sound waves exists in potassium, and that there is good agreement of the theory with experiment.

It is a pleasure to acknowledge the technical assistance of G. Adams. Miss B. B. Cetlin computed the theoretical curves.

¹P. Aigrain, Proceedings of the International Conference on Semiconductor Physics, Prague, 1960 (Czechoslovakian Academy of Sciences, Prague, 1961), p. 224; R. Bowers, C. Legendy, and F. Rose, *Phys. Rev. Letters* **7**, 339 (1961).

²G. Akramov, *Fiz. Tverd. Tela* **5**, 1310 (1963) [translation: *Soviet Phys.-Solid State* **5**, 955 (1963)].

³T. Kjeldaas, Jr., *Bull. Am. Phys. Soc.* **8**, 428, 446 (1963); and private communication (to be published).

⁴D. N. Langenberg and J. Bok, *Phys. Rev. Letters* **11**, 549 (1963); J. J. Quinn and S. Rodriguez, *Phys. Rev. Letters* **11**, 552 (1963); *Phys. Rev.* **133**, A1589 (1964).

⁵T. Kjeldaas, Jr., *Phys. Rev.* **113**, 1473 (1959); M. H. Cohen, M. J. Harrison, and W. A. Harrison, *Phys. Rev.* **117**, 937 (1960).

⁶At 4.2°K the approximate value of $\omega_c\tau$ where ω_c is the electron cyclotron frequency ranged from 70 to 220 at the magnetic fields employed in the experiments.

⁷Previous experimental arrangements used on metals have allowed only observation of standing-wave resonances corresponding to an odd number of half-wavelengths contained in the specimen [F. E. Rose, M. T. Taylor, and R. Bowers, *Phys. Rev.* **127**, 1122 (1962); R. G. Chambers and B. K. Jones, *Proc. Roy. Soc. (London)* **A270**, 417 (1962)]. Our traveling-wave experimental technique is readily extended to much higher frequencies than can be employed using the standing-wave technique. The cyclotron damping effects first observed by Taylor, Merrill, and Bowers [M. T. Taylor, J. R. Merrill, and R. Bowers, *Phys. Letters* **6**, 159 (1963)] are more clearly resolved using the traveling-wave technique at high frequencies and will be discussed in a future publication.

⁸The calculated phase velocities of the two shear waves which propagate in the [110] direction in potassium are 0.67×10^5 cm/sec and 1.70×10^5 cm/sec. Here we have used the elastic constants listed by Mason [W. P. Mason, Physical Acoustics and the Properties of Solids (D. Van Nostrand Company, Inc., Princeton, New Jersey, 1948)] and the lattice constant measured by Barrett [C. S. Barrett, *Acta Cryst.* **9**, 671 (1956)] at 5°K.

NONEXTREMAL ORBITS IN MAGNETOACOUSTIC GEOMETRIC RESONANCES*

S. G. Eckstein

Argonne National Laboratory, Argonne, Illinois

(Received 17 February 1964)

In a recent Letter, Langenberg, Quinn, and Rodriguez¹ discussed the possibility of measurement of nonextremal Fermi-surface orbits by observing giant quantum oscillations in the attenuation of sound, for sound waves parallel to the direction of the magnetic field. In this Letter we wish to point out that these same nonex-

tremal orbits (as well as other nonextremal orbits) may also be observed in geometric resonance experiments, and furthermore, the conditions for observation of these orbits are much easier to attain in the case of geometric resonance than in the quantum oscillation case. Since geometric resonances measure linear dimensions